The Pharmaceutical and Chemical Journal, 2017, 4(3):46-54

Available online www.tpcj.org

Research Article

ISSN: 2349-7092
CODEN(USA): PCJHBA

Synthesis and Comparison Spherical and Bars Iron Oxide Nanoparticles: Providing Reaction Mechanisms

Rana Khalilnezhad[1], Azam Pirkarami*[2], Leila Fereidooni[3]

[1]Department of Chemistry, Tehran medical Branch, Islamic Azad University, Tehran, Iran
[2]Department of Nanomaterials & Nanocoatings, Institute for Color Science and Technology (ICST), Tehran, Iran
[3]Young Researchers and Elites Club, Islamic Azad University, North Tehran Branch, Tehran, Iran

Abstract Nanomaterials, especially inorganic nanomaterials such as metal, metal oxide, metal sulfate, quantum dots, et al. With the basic properties of quantum dots significantly in the development of biomedical, catalytic, fuel cells, sensors and magnetic data storage were attracted. The term nano-crystal can be designed and synthesized nano-crystal morphology and composition to the understanding and extraction of nucleation and growth processes to be defined. The process of nano-materials in biomedical applications, catalysis, fuel cells and solar and magnetic data storage is key. This paper presents a comprehensive review of inorganic nanomaterials with controlled of germination and growth through the theory of controlled laboratory conditions, provide a brief account of the control of nano-iron oxide minerals during the synthesis process provides more chemistry. Moreover, similar mechanisms for control of nano-minerals are also clearly described. Spherical and rod iron oxide nanoparticles synthesized by co-precipitation and hydrothermal processes were examined. Then the FT-IR and SEM techniques were studied.

Keywords Iron oxide, co-precipitation, hydrothermal, Classical nucleation, Classical growth

1. Introduction

Nanomaterials, especially inorganic nanomaterials such as metal, metal oxide, metal sulfate, quantum dots, et al. With the basic properties of quantum dots significantly in the development of biomedical, catalytic, fuel cells, sensors and magnetic data storage were attracted [1-3]. Over the past two or three decades advances in the synthesis of inorganic nano-materials and exploring their applications have been transformative. In the range of nanoscale inorganic particles, shape they can be in the form of zero-dimensional (isotropic structure), one-dimensional, two-dimensional and three-dimensional (anisotropic structure) classified. In the case of inorganic nanoparticles zero-dimensional forms typically include: Spherical, semi-spherical, hexagonal, octagonal, square and morphology of their respective hollow structure. One-dimensional morphology of inorganic nanoparticles include: Nanotubes, nanorods and nanowires, nano-shuttle, nano-capsules, hollow structures, etc. [4-5]. Round disk, triangular, hexagonal, quadrangular plates or sheets, belts, mesoporous- hollow nanosphere, hollow rings, etc. belong to dimensional shape of inorganic NPs [6]. Three-dimensional morphology of inorganic nanoparticles complex that includes: Needle-shaped nano-structures, nano-flower, nano-star, nano-frame, multi-shell nanoparticles hollow, hollow and so are clusters [7-8]. In recent decades more effort into controlling the formation of inorganic nanoparticles and further advances in the synthesis of inorganic nanoparticles with controlled shape and form was dependent properties. In general, the formation of inorganic nano-particles kinetic or thermodynamic control behavior can be changed or controlled in solution. Naturally thermodynamic control the morphology of nanoparticles with potential mine when done the chemical reaction goes forward reaction solution is directly

dependent on the temperature and the solution is supersaturated. The synergistic effect of Thermodynamics and Kinetics aspects play an important role in determining the final shape of inorganic particles are nano [11].

In this research, nanoparticles of iron oxide spherical and rod was synthesized. Also by SEM and FTIR techniques were studied. It is worth noting that no simple rule for determining the final form of Fe_3O_4 does not exist. The general rule germination and growth that normally occurs in solution mass and the corresponding reaction in all reaction parameters include: Precursors or the supersaturation concentration, reaction temperature, storage time and additives were not considered yet. So as to achieve a comprehensive understanding of the formation mechanism and method for forming nanoparticles Fe_3O_4, The effects of the reaction parameters during the process of Fe_3O_4 nanoparticles have been studied. The usual mechanisms for Fe_3O_4 nanoparticles with controlled shape is to provide guidance for further research.

2. Materials and Methods

2.1. Hydrothermal techniques and materials used in the hydrothermal method for the synthesis of iron oxide nanoparticles bar

The word hydrothermal largely heterogeneous reaction in the presence of any aqueous solvent at temperatures above the critical temperature and high pressure, resulting in the shed. In other words, hydrothermal synthesis under the influence of temperatures above 100 ° C and atmospheric pressure higher than a shed. With increasing pressure on the system, can be at a higher temperature than normal boiling point material, kept in a liquid state. Water is the safest and cheapest type of solvent in hydrothermal processes under conditions of high temperature and pressure can act as a catalyst. Stability and particle size of the final product to the amount and concentration of catalyst, temperature and reaction time will depend. Hydrothermal method to synthesize in a laboratory scale autoclave is used mainly depending on the type of process has several types. In this process of hydrothermal method for the synthesis of nanoparticles of Fe_3O_4 rods were used. In this experiment, 0.5 gr surfactant (CTAB) were dissolved in deionized water 40 cc. Of iron nitrate Fe $(NO_3)_3 \bullet 9H_2O$ 89% Merck. Merck added 50 cc n-hexane. Coordination solvents with different functional groups has specific precursors of iron oxide brings for forming nanoparticles of iron oxide under the control of thermodynamics or kinetic rod for arranging increase or decrease the speed advantage is supersaturated. In addition, different solvents or solvent mixtures with different combinations makes it possible to control the shape of nanoparticles of iron oxide. Combine 1.5 g of urea, poured in an autoclave and the temperature was 160 $^{\circ}$C for 8 hours. Process pH 3.5 was initially released with time and OH^- urea solution pH was 9.5. Surface properties of Fe_3O_4 nanoparticles and the physical and chemical surfactants (CTAB) or to regulate additives that lead to different absorption or adsorption on the surface of the Fe_3O_4 nanoparticles. As a result of selective growth, accumulation and concentration for the development of nano-particles spherical and rod of Fe_3O_4 is favorable.The benefits of this approach in the purity and homogeneity of the product, the symmetry of crystals, narrow particle size distribution, chemical composition, use or production of a wide range, single-step processes, to produce nanoparticles of different size, low power consumption and residence time.

2.2. The materials used in the Co-precipitation process for synthesizing spherical iron oxide nanoparticles

In this process of co-precipitation method for the synthesis of spherical Fe_3O_4 nanoparticles were used. In this experiment, 5 g of zinc nitrate were dissolved in 100 cc of deionized water. As drop by drop in a molar NaOH was added. Until the solution is dark brown. The pH was adjusted to 8. pH modulation mode changes to the chemical species in solution and concentration bonds with Fe_3O_4 precursor ions in solution to form the complex. Finally, upgrade or delay the rate of release of ions from concentration bond to oversaturation, set the pace early germination enables shape control. The process was given one hour to precipitate. Were dried at 90 °C and the spherical Fe_3O_4 particles were separated with a filter paper. Then put in the oven at 700 °C to remove organic impurities.

2.3. Evaluation of treatment efficiency

The samples were mixed with spectroscopically pure KBr in the ratio of 3:100 to make pellets, which were then placed in the Shimadzu 8300 FT-IR (Perkin-Elmer, Spectrum one). FT-IR spectroscopy was performed in the range of 450 to 4000 cm^{-1} for the study of spherical and rod Fe_3O_4 nanoparticles. The morphological features and surface characteristics of Fe_3O_4 were studied using a scanning electron microscope (SEM) unit (HITACHI-3000 SH Model, Japan).

3. Results and Discussion

3.1. Classical Nucleation

The definition and classification of germination by clients since 1961 is described so that the germination process which caused the second phase of a phase [14]. In solution and solid particles that are considered as the second phase of the solution phase precursor to have been created by the germination process. Here, if the nuclei produced solid supersaturated solution homogeneous pile, to be considered as primary sprouts. In contrast, if new sprouts produced in pile supersaturated solution in the presence of other substances or particles with the same and different components (e.g. container, surfaces, impurities and grain boundaries) respectively as secondary nuclei and called heterogeneous nucleation. In addition, the heterogeneous nucleation and secondary nucleation is much easier than primary because germination due to low energy barrier system is stable nucleation sites. As reported by Mullin, [14] and other researchers [15] is provided, uniform nuclei formation as a thermodynamic process using a solution of super-saturation pile and total free energy (ΔG) for total iron oxide nanoparticles free energy surface free energy and mass (ΔG_V) is considered. As shown in Equation 1.

$$\mathbf{\Delta G = 4\pi r^2 y \frac{4}{3}\pi r^3 \Delta G_V} \quad (1)$$

Where r and y are respectively the radius of the particle and energy level. As regards of the free energy of bulk crystal ΔG_V is defined as free energy change of transformation to unit volume of particles, dependent upon temperature T, Boltzmann's constant kB , its molar volume v, and supersaturation ratio of bulk solution S. That is, $\mathbf{\Delta G_V = \frac{-2y}{r} = \frac{-2k_B T \ln(s)}{v}}$. Especially S as the ratio of monomer concentration in the crystal in a solution of C to C * is the equilibrium monomer concentration (S = C / C *). The germination process in homogeneous solution with increased spending free energy to form the interface between pile solution and solid surface germ is carried out. Nuclei are formed with a radius depends to a large extent on the level of saturated and supersaturated quickly increase and narrow distribution, led to a small particle size is defined as the energy released ΔG_V mass. The critical value of ΔG and critical radius of nuclei that existed in the bulk solution is conducted by differentiating ΔG with respect to radius r when ΔG is set to zero, $\mathbf{d(\Delta G_{crit})/dr = 0}$giving a critical free energy in Eq. 2. Apparently, $\mathbf{\Delta G_{crit}^{homo}}$is required to obtain stable nuclei within solution (Figure 1) [16-18].

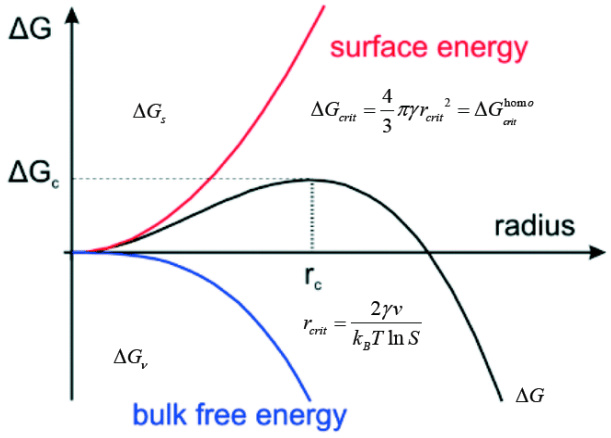

Figure 1: Relationship of energy with radius

The critical radius of at least the size of the nuclei remaining in the solution without being re-defined in Equation 3 is solved.

$$\Delta G_{crit} = \frac{4}{3}\pi y r_{crit^2} = \Delta G_{crit}^{homo} \quad (2)$$

$$r_{crit} = \frac{-2y}{\Delta G_V} = \frac{2yv}{k_B T \ln S} \quad (3)$$

A nucleation rate of nuclei N formed per unit time per unit volume, were written in a form of Arrhenius reaction velocity equation, which is commonly used for the rate of a thermally active process:

$$\frac{dN}{dt} = Aexp(-\frac{\Delta G_{crti}}{K_B T}) = A_{exp}(\frac{-16\pi y^3 v^2}{3k_B^3 T^3 (\ln S)^2}) \quad (4)$$

Where A is an exponential factor. Monomer concentration, high temperature and lower critical energy levels are favourable for rapid germination. Leading to high population nuclei with small size, as shown in a large number of synthesis processes [19, 20].

3.2. Classical growth and dissolution

After nucleation subsequent growth of nuclei is strongly determined the shape of nanomaterials, which is thermodynamically driven by the decreasing surface free energy of generated particles. The growth of primary sedimentation (including atoms, molecules, or aggregates of particles) that binds to the nanoparticles formed in the growth environment (plasma, liquid, solution, gel etc.). The connection surface in places nuclei occur. Density locations nuclei are formed on the surface along with the kinetics of places now have an important role in determining the growth rate nanoparticles [21]. In classical growth theory, there are two growth mechanisms, including the response surface [22] and influence monomers to the surface particle [21]. As described Fick's first law of influence is, if the flux of monomers from the surface of spherical particles with a radius x, speed monomers influence through these levels can be written as follows:

$$\frac{dm}{dt} = JA = -4\pi x^2 D \frac{dC}{dx} \quad (5)$$

where J is monomer flux and D is diffusion constant. The diffusion rate of monomers at spherical NPs surface with radius r at steady state, the above equation can be written as

$$\frac{dm}{dt} = 4\pi x r D(C_b - C_i) \quad (6)$$

Where C_b monomer concentration in solution mass, C_i monomer concentration at the interface of solid / liquid. Similarly, the equations can be written for surface reaction rate:

$$\frac{dm}{dt} = 4\pi r^2 k(C_b - C_i) \quad (7)$$

Where k mass transfer coefficient, C_r equilibrium concentration of nanoparticles is solid.

If influence limiting factor and particle size changes with time, the influence monomer on the surface of nanoparticles is given in Equation (8).Similarly, if the reaction surface is a limiting factor in the equation 7 can be written as Equation 9.

$$\frac{dm}{dt} = \frac{Dv}{r}(C_b - C_i) \quad (8)$$

$$\frac{dr}{dt} = kv(C_b - C_i) \quad (9)$$

Where Cr solubility of nanoparticles and nanoparticles v is the molar masses. Two factors limiting the growth of nanoparticles by the penetration or surface reaction control and then increase in size with time is shown in Equation 10:

$$\frac{dm}{dt} = \frac{Dv}{r+D/k}(C_b - C_i) \quad (10)$$

A plan of concentration as the driving force for diffusion and reaction crystal growth shown in Figure 2. Diffusion-limited or reaction-limited process with different concentration of precursor monomer determines the shape of nano-particles by growth rate [23]. The precursor solution with high concentrations of soluble monomeric growth rate is limited to influence processes controlled. The influence rate determining step is a precursor monomer. The precursor monomer immediately on the surface of nanoparticles through the mass reaction and solvent can be precipitated. However, in the case of reaction-limited growth process, when concentration of precursor monomer is low and

progress is greatly restricted to surface reaction of monomers, total growth rate is identified by the relative nucleation and growth rate of monomers on surface of nanoparticles.

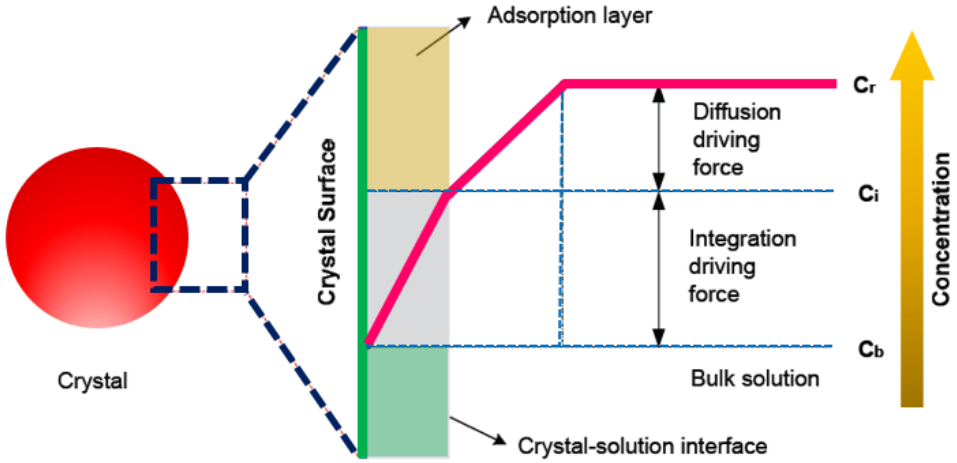

Figure 2: Diffusion model - the growth of crystals with concentrations in solution

Normally limited to influence growth process is suitable for producing nanoparticles with a uniform distribution. But growth is limited to the reaction, determines the final shape of the nanoparticles. Throughout the diffusion-limited growth process, organic ligands or surfactants adsorbed on the surface of performed nanoparticles introducing the diffusion barrier is a flexible and effective strategy to get handled condition with monodisperse size.

3.3. A cursory reading of the spherical and rod quasi Fe_3O_4nanoparticles by SEM techniques

Fe_3O_4 morphology of was evaluated by SEM in Co-precipitation and hydrothermal processes. Figure (Figure 3a) shows nanoparticles accumulate bar adjacent particles spontaneously self-orientation and continuous growth Fe_3O_4 particles self-organized rod is at an early stage. The self-organized particle encapsulation share a common crystallographic take sides and as specified in the form of a flat subscription level to come together. During this process, fusion between nanoparticles composed of the driving force is to share crystallographic take sides.Although this fusion that leads to the crystallographic take sides can be affected by other factors led to the formation of crystals in the reaction solution can be oriented hybrid ISO, meso-crystal and single crystal from different directions to be. Reasonable explanation for the occurrence of "OA" Fe_3O_4 particles rods that connect to the encapsulation of particles in high-energy funds to remove surface energy can be done. After such a connection, the removal of these funds with high energy and fusion in crystallography, the second full anisotropic particles. During the middle stages of OA may be related to the collision or processes of accumulation and density. Present research suggests that treatment of OA may be promiscuous or rotating nano-crystals orientation in the suspension of nanoparticles in contact with common surfaces with low energy configuration occur [24]. Regarding spontaneous self-organization of adjoining particles and continuous regarding the self-organized particles at initial step. Then, the self-organized particles share one common crystallographic orientation and join at a planar interface. (Figure 3b) shows a semi-spherical Fe_3O_4 nanoparticles have been synthesized by co-precipitation process. As the picture is clear spherical particles does not appear perfectly spherical Fe_3O_4. For reasons that may be causing a problem uniformity spherical nanoparticles Fe_3O_4: aggregation and agglomeration of Fe_3O_4 nanoparticles cause changes in the morphology of the particles are spherical. Accumulation of nanoparticles is a complex phenomenon that creates form to deal in their properties and applications of nano-structured materials to be [25]. Common reasonable explanation for the aggregation of nanoparticles is their high surface free energy. So a direct attraction between particles (such as van der Waals forces or chemical bonding) to assemble nanoparticles are formed through such movement and gravity [26]. May accumulate in the reaction solution with high concentrations of nanoparticles Fe_3O_4, and stirring rate does

not occur. Aggregation of spherical nanoparticles of iron oxide nanoparticles may be due to incomplete drying is to SEM techniques.

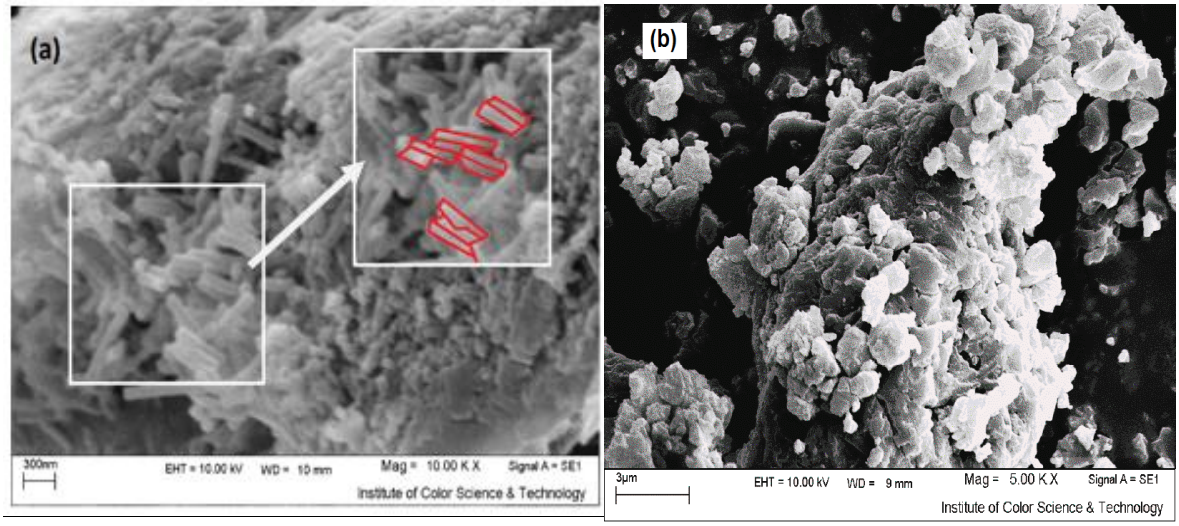

Figure 3: SEM images of nanoparticles of iron oxide rods by hydrothermal method, (a) quasi-spherical iron oxide nanoparticles by co-precipitation method (b).

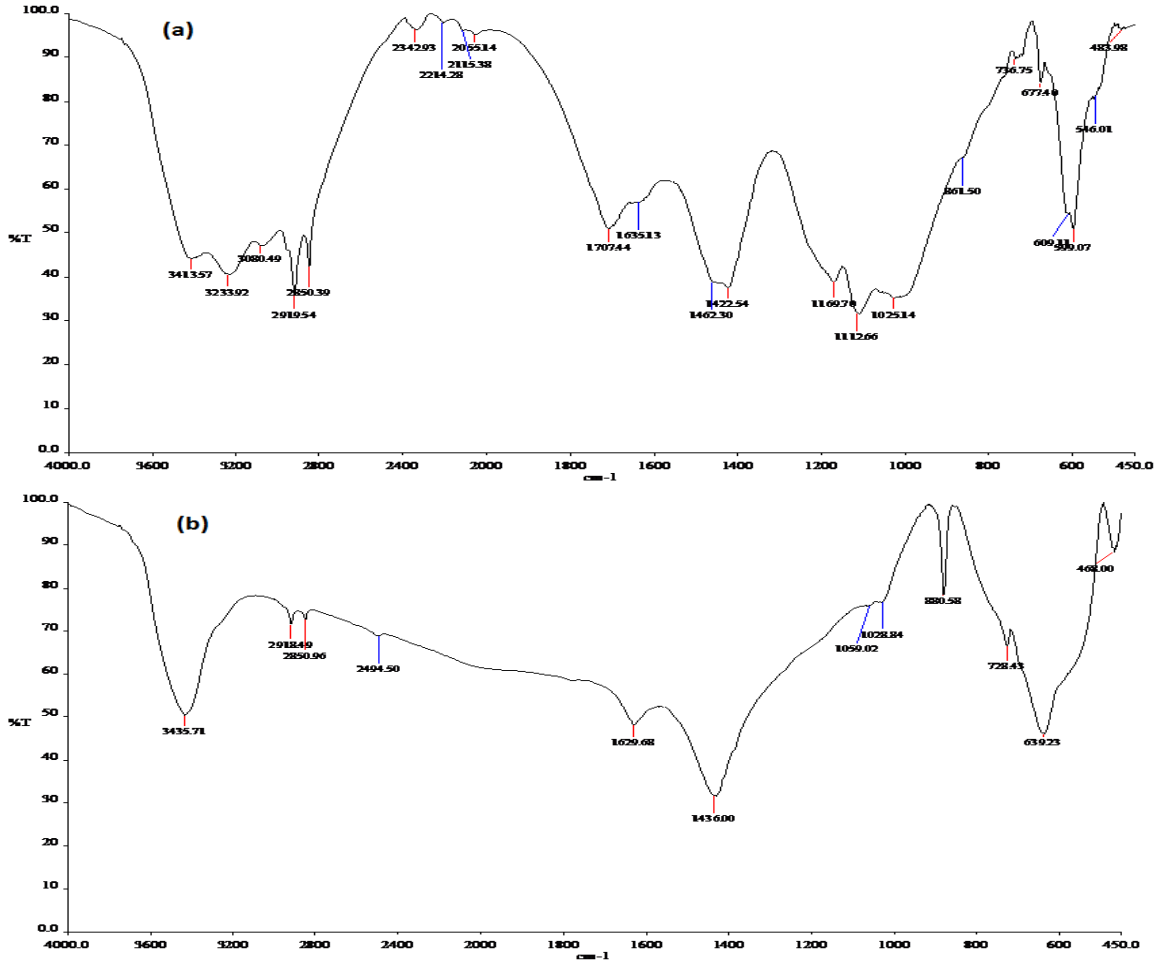

Figure 4: FT-1R spectrum rod of iron oxide nanoparticles by hydrothermal method, (a) spherical iron oxide nanoparticles by co-precipitation method (b).

3.4. FT-IR Spectral Analysis

Spherical iron oxide nanoparticles synthesized efficiency ratio and bars can be identified by FT-IR spectra (Figure 4-a). Can be see that some structural changes in the spherical iron oxide nanoparticles synthesized by hydrothermal method and co-precipitation rod occur. (Figure 4-a) FT-IR whole rod of Fe_3O_4nanoparticles show. Appearing on Spectrum 3413 cm^{-1} group NH_2, in 3233 cm^{-1} group NO_2.In 2919 cm^{-1} group CTAB Fe^{2+} [27], 2850 cm^{-1} also represents the group CH_2-CH_2 group n- hexane. The disappearance of spectrum 2115 cm^{-1} and 2055 cm^{-1} and that of symmetric and asymmetric carbonyl, That's because the interaction between the groups of Fe (NO_3). In 2115, 2707, 1422-1462 cm^{-1} shows by groups, C-N, C≡N, C=O, and urea [28], (Figure 4-b) FT-IR Spectrum shows spherical nanoparticles of Fe_3O_4 to co-precipitation method.3434 cm^{-1} dedicated to stretching and vibration level OH, 2850-2918 cm^{-1}, shows C-H groups. 1436 cm^{-1} CH_2 and CH_3 flexural vibration represents the groups. 1629 cm^{-1} also representative of the group C-N in spherical nanoparticles of iron oxide.639 and 463 cm^{-1} respectively show that Fe-O and Fe-C in the process. Stability of nanoparticles of spherical and rod with co-precipitation method and hydrothermal method can be studied.

Conclusion

Many more efforts to synthesize nano-minerals has been conducted uniformly and customizable. Figure controlled mineral nanoparticles in addition to their inherent physical and chemical properties of nano applications of new technology in the field of biomedical, catalytic, electronic,and optical, etc. is introduced.This article is a brief review of the classical theory and factors affected germination and growth and generally acceptable mechanisms to control the germination and growth of nano-inorganic particles in order to provide theory.

At first the basic concepts of classical crystallization theory and general agents to control the germination and growth was explained. Despite the overall effect that is listed parameters, process complex and easily influenced by many factors reaction that leads to uncertain factors in controlling the formation of inorganic nanoparticles. So the reaction process and its parameters should be appropriately controlled. Spherical and rod iron oxide nanoparticles synthesized by co-precipitation and hydrothermal processes were examined. Then the FT-IR and SEM techniques were studied and observed, in this study were not perfectly spherical Fe_3O_4 spherical nanoparticles and the surface tension may be due to accumulation of nanoparticles, the choice of surfactants and additives, dry incomplete nanoparticles, high concentrations of nanoparticles Fe_3O_4, and stirring rate it happened .

References

1. Seifert, G.; Stalmashonak, A.; Hofmeister, H.; Haug, J.; Dubiel, M., Laser-induced, polarization dependent shape transformation of Au/Ag nanoparticles in glass. Nanoscale Res. Lett. 2009, 4 (11), 1380-1383.
2. Buonsanti, R.; Grillo, V.; Carlino, E.; Giannini, C.; Gozzo, F.; Garcia-Hernandez, M.; Garcia, M. A.; Cingolani, R.; Cozzoli, P. D., Architectural control of seeded-grown magnetic-semicondutor iron oxide-TiO_2 nanorod heterostructures: The role of seeds in topology selection. J. Am. Chem. Soc. 2010, 132 (7), 2437-2464.
3. Wu, W.; Jiang, C. Z.; Roy, V. A. L., Recent progress in magnetic iron oxide–semiconductor composite nanomaterials as promising photocatalysts. Nanoscale 2015, 7, 38-58.
4. Chang, W. G.; Shen, Y. H.; Xie, A. J.; Liu, X., Facile controlled synthesis of micro/nanostructure $MCrO_4$ (M = Ba, Pb) by using Gemini surfactant C12-PEG-C12 as a soft template. Appl. Surf. Sci. 2010, 256 (13), 4292-4298.
5. Khan, Z.; Al-Nowaiser, F. M., Effect of poly(vinyl alcohol) on the size, shape, and rate of silver nanoparticles formation. J. Disper. Sci. Technol. 2011, 32 (11), 1655-1660.
6. Li, X. L.; Zhang, F. Q.; Ma, C.; Deng, Y.; Wang, Z. F.; Elingarami, S.; He, N. Y., Controllable synthesis of ZnO with various morphologies by hydrothermal method. J. Nanosci. Nanotechno. 2012, 12 (3), 2028-2036.

7. Lv, H. L.; Ji, G. B.; Liu, W.; Zhang, H. Q.; Du, Y. W., Achieving hierarchical hollow carbon@Fe@Fe_3O_4 nanospheres with superior microwave absorption properties and lightweight features. J. Mater. Chem. C 2015, 3 (39), 10232 10241.
8. Lin, X. H.; Ji, G. B.; Liu, Y. S.; Huang, Q. H.; Yang, Z. H.; Du, Y. W., Formation mechanism and magnetic properties of hollow Fe3O4 nanospheres synthesized without any surfactant. Cryst. Eng. Comm. 2012, 14 (24), 8658-8663.
9. Ho, C. H.; Tsai, C. P.; Chung, C. C.; Tsai, C. Y.; Chen, F. R.; Lin, H. J.; Lai, C. H., Shape-controlled growth and shape-dependent cation site occupancy of monodisperse Fe3O4 nanoparticles. Chem. Mater. 2011, 23 (7), 1753-1760.
10. Radi, A.; Pradhan, D.; Sohn, Y.; Leung, K. T., Nanoscale shape and size control of cubic, cuboctahedral, and octahedral Cu-Cu2O core-shell nanoparticles on Si(100) by one-step, templateless, capping-agent-free electrodeposition. ACS Nano 2010, 4 (3), 1553-1560.
11. Zhang, H.; Jin, M. S.; Xiong, Y. J.; Lim, B.; Xia, Y. N., Shape-controlled synthesis of Pd nanocrystals and their catalytic applications. Acc. Chem. Res. 2013, 46 (8), 1783-1794.
12. Do, T. O.; Nguyen, T. D.; Dinh, C. T., A general procedure to synthesize highly crystalline metal oxide and mixed oxide nanocrystals in aqueous medium and photocatalytic activity of metal/oxide nanohybrids. Nanoscale 2011, 3 (4), 1861-1873.
13. Chang, J.; Waclawik, E. R., Colloidal semiconductor nanocrystals: controlled synthesis and surface chemistry in organic media. RSC Adv. 2014, 4 (45), 23505-23527.
14. Mullin, J. W., Crystallization. 4th ed.; Butterworth-Heinemann: Oxford; Boston, 2001, 594.
15. Thanh, N. T. K.; Maclean, N.; Mahiddine, S., Mechanisms of nucleation and growth of nanoparticles in solution. Chem. Rev. 2014, 114 (15), 7610-7630.
16. Gilroy, K. D.; Hughes, R. A.; Neretina, S., Kinetically controlled nucleation of silver on surfactant-free gold seeds. J. Am. Chem. Soc. 2014, 136 (43), 15337-15345.
17. Min, Y.; Kwak, J.; Soon, A.; Jeong, U., Nonstoichiometric nucleation and growth of multicomponent nanocrystals in solution. Acc. Chem. Res. 2014, 47 (10), 2887-2893.
18. Sun, Y. G., Controlled synthesis of colloidal silver nanoparticles in organic solutions: empirical rules for nucleation engineering. Chem. Soc. Rev. 2013, 42 (7), 2497-2511.
19. Wagle, D. V.; Zhao, H.; Baker, G. A., Deep eutectic solvents: Sustainable media for nanoscale and functional materials. Acc. Chem. Res. 2014, 47 (8), 2299-2308.
20. Sun, W.; Liu, H.; Hu, J. C.; Li, J., Controllable synthesis and morphology-dependent photocatalytic performance of anatase TiO_2 nanoplates. RSC Adv. 2015, 5 (1), 513-520.
21. Sugimoto, T., Monodispersed Particles. Elsevier B.V. Amsterdam, 2001.
22. Sugimoto, T.; Zhou, X. P.; Muramatsu, A., Synthesis of uniform anatase TiO_2 nanoparticles by gel-sol method: 3. Formation process and size control. J. Colloid Interf. Sci. 2003, 259 (1), 43-52.
23. Zong, R. L.; Wang, X. L.; Shi, S. K.; Zhu, Y. F., Kinetically controlled seed-mediated growth of narrow dispersed silver nanoparticles up to 120 nm: secondary nucleation, 807 size focusing, and Ostwald ripening. Phys. Chem. Chem. Phys. 2014, 16 (9), 4236-4241.
24. Lee, E. J. H.; Ribeiro, C.; Longo, E.; Leite, E. R., Oriented attachment: An effective mechanism in the formation of anisotropic nanocrystals. J. Phys. Chem. B 2005, 109 (44), 20842- 20846.
25. Noorduin, W. L.; Vlieg, E.; Kellogg, R. M.; Kaptein, B., From Ostwald ripening to single chirality. Angew. Chem. Int. Ed. 2009, 48 (51), 9600-9606.
26. Joo, S. H.; Park, J. Y.; Tsung, C. K.; Yamada, Y.; Yang, P. D.; Somorjai, G. A., Thermally stable Pt/mesoporous silica core-shell nanocatalysts for high-temperature reactions. Nat. Mater. 2009, 8 (2), 126-131.
27. Liu XH, Luo XH, Lu SX, Zhang JC, Cao WL. A novel cetyltrimethyl ammonium silver bromide complex and silver bromide nanoparticles obtained by the surfactant counterion. J Colloid Interface Sci. 2007 Mar 1; 307(1):94-100.

28. Le Caër S, Vigneron G, Renault JP, Pommeret S. First coupling between a LINAC and FTIR spectroscopy: the aqueous ferrocyanide system. Chem Phys Lett. 2006; 426:71–76.